An Investigation of the Scattering of Surface Waves at Dielectric Slab Waveguide with Axial Discontinuity

CRESO S. DA ROCHA [1]

Abstract— **This paper introduces a technique for studying the radiation due to an abrupt axial discontinuity in the geometry of a planar dielectric waveguide (slab waveguide) when an even TM surface wave strikes the discontinuity. The mode matching technique is applied at the discontinuity giving rise to formally exact integral equations which are solved by the Method of Moments.**

I. Introduction

ELECTROMAGNETIC scattering due to a discontinuity in the geometry of a surface waveguide has occupied attention of several investigators in the past few decades [1]-[7]. These authors, in one way or another, make approximations that turn solution of the problem unavailable for large range of discontinuity. On the other hand, in all cases, the back radiation is considered very small and neglected. In our work there is no restriction values for the discontinuity, but we can observe that the solution becomes unstable as the structure in the right side approaches the air, Fig. 1, (by making $b_2 = 0$).

In this paper a method for investigating the scattering of an incident surface wave at the axial discontinuity of a dielectric slab with a step in the geometry is introduced. In our approach we formulate the field equations in an exact way by using the mode matching technique of the tangential fields, represented by a complete set of eigenfunctions that are solved by the Method of Moments. In the integral equations, both back and forward scattered radiation spectral densities are considered, initially without approximations.

II. Mode Matching at the Interface

With reference to Fig. 1, consider a TM surface wave with even symmetry $[H_y(x) = H_y(-x)]$ striking the discontinuity at $z = 0$ from the left and giving rise to a transmitted and a reflected surface wave as well as scattered radiation. The single mode is guaranteed by taking the slab of thickness not larger than $2b_c$ in the region I, where b_c is given by $2b_c = \lambda_0/\sqrt{\epsilon_r - 1}$ (dominant mode). At the discontinuity the boundary conditions cannot be satisfied by the surface waves alone; an additional field with radiation characteristics must be introduced, that is, the total field must be given as

$$\psi_1 = \psi_{incident} + \psi_{reflected} + \psi_{radiated}, \quad [z \leq 0]$$

and

$$\psi_2 = \psi_{transmitted} + \psi_{radiated}, \quad [z \geq 0]$$

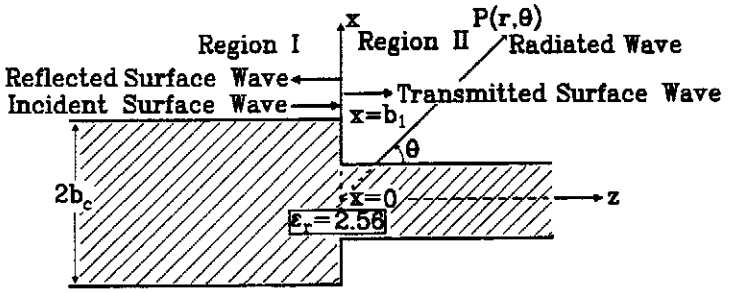

(a) The slab waveguide with abrupt step in the geometry

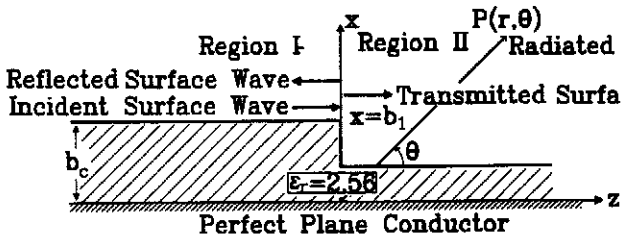

(b) Equivalent Structure for even TM_0 mode

Figure 1: The Dielectric Slab with Axial Discontinuity.

The radiation is accounted for by the continuous spectrum of pseudo-surface waves. Because $h(s)$, the wave number in the $z-$direction for the continuous spectrum, is a double-valued function of s, the wave number in the $x-$direction, it is necessary to define its branches to uniquely define the pseudo-mode solutions, that is

$$h(s) = +\sqrt{k_0^2 - s^2}, \quad [0 \leq s \leq k_0] \qquad (1)$$

$$h(s) = -j\sqrt{s^2 - k_0^2}, \quad [k_0 \leq s \leq \infty] \qquad (2)$$

[1] The author is with the Department of Electrical Engineering, Federal University of Paraíba, P.O. Box 10053 - 58100 Campina Grande, PB - Brazil, **e-mail**: creso@dee.ufpb.br

Equation (1) corresponds to the spectrum of radiation modes (visible range) while equation (2) is for the evanescent modes (invisible range).

Let the incident surface wave have amplitude I and the reflected and transmitted surface waves have amplitude R and T, respectively. Taking $\psi = H_y(x,z)$ for the TM_0 mode. Matching the total fields at $z=0$ gives [8]

$$(I+R)h_{y1} + \int_0^\infty [B_1(s)/h(s)]h_{y1}(s)ds = Th_{y2} + \int_0^\infty [B_2(s)/h(s)]h_{y2}(s)ds \quad (3)$$

$$(h_1/\epsilon_{r1})(I-R)h_{y1} - \int_0^\infty (1/\epsilon_{r1})B_1(s)h_{y1}(s)ds = (h_2/\epsilon_{r2})Th_{y2} + \int_0^\infty (1/\epsilon_{r2})B_2(s)h_{y2}(s)ds \quad (4)$$

where h_y and $h_y(s)$ are the transverse function for the discrete and continuous TM field, respectively. B_1 and B_2 are the unknown spectral densities for the left and right region, respectively. In the expressions above, including the dielectric constant, the x–dependence is understood.

III. Transformation to the Spectral Domain

In order to apply the Moment Method one must first eliminate the x–dependence, so that (3) and (4) will be in a form suitable for computation. To do so and to take advantage of the orthogonality properties, (3) is multiplied by $h_{y1}(\tilde{s})/\epsilon_1(x)$ and by $h_{y1}/\epsilon_1(x)$ separately and integrated over x from 0 to ∞ [8]. Similarly (4) is multiplied by $h_{y1}(s)$ and h_{y1} separately and integrated over x from 0 to ∞.

Noting the orthogonality properties, the following set of equations is obtained:

$$\frac{B_1(\tilde{s})}{h(\tilde{s})}N_1^2(\tilde{s}) = TF_{12}(\tilde{s}) + \int_0^\infty B_2(s)H_{12}(s,\tilde{s})ds/h(s) \quad (5)$$

$$-B_1(\tilde{s})N_1^2(\tilde{s}) = h_2TG_{12}(\tilde{s}) + \int_0^\infty B_2(s)I_{12}(s,\tilde{s})ds \quad (6)$$

$$(I+R)N_1^2 = TH_{12} + \int_0^\infty B_2(s)G_{21}(s)ds/h(s) \quad (7)$$

$$(I-R)h_1N_1^2 = h_2TI_{12} + \int_0^\infty B_2(s)F_{21}(s)ds \quad (8)$$

where the integrals $F_{12}(\tilde{s})$, $G_{12}(\tilde{s})$, $H_{12}(s,\tilde{s})$, $I_{12}(s,\tilde{s})$, $F_{21}(s)$, $G_{21}(s)$, H_{12} and I_{12} and the normalization factors N_1 and $N_1(s)$ are defined as follows, for i and j mutually exclusive and equal to 1 or 2 according to the region considered (left or right region):

$$F_{ij}(\tilde{s}) = \int_0^\infty \frac{1}{\epsilon_i(x)}h_{yi}(\tilde{s})h_{yj}dx \quad (9)$$

$$H_{ij}(s,\tilde{s}) = \int_0^\infty \frac{1}{\epsilon_i(x)}h_{yi}(\tilde{s})h_{yj}(s)dx \quad (10)$$

$$H_{ij} = \int_0^\infty \frac{1}{\epsilon_i(x)}h_{yi}h_{yj}dx \quad (11)$$

$$N_i^2 = \frac{1}{2}\left[\frac{b_i}{\epsilon_i} + \frac{\sin(2g_ib_i)}{2\epsilon_ig_i} + \frac{\cos^2(g_ib_i)}{\alpha_i}\right] \quad (12)$$

and

$$N_i^2(s) = \frac{\pi}{2}\left[v_i^2(s) + w_i^2(s)\right] \quad (13)$$

where $v_i(s)$ and $w_i(s)$ are defined as follows ([8], Cap. 2):

$$v_i(s) = \cos[g_i(s)b_i] \quad (14)$$

$$w_i(s) = \frac{g_i(s)}{\epsilon_{ri}s}\sin[g_i(s)b_i] \quad (15)$$

g_i is the discrete wavenumber inside the guide and α_i is an attenuating factor outside the guide in x–direction. Note the g_i and α_i are solutions of the characteristic equation system

$$g_i\tan(g_ib_i) = \alpha_i\epsilon_{ri}$$

$$g_i^2 + \alpha_i^2 = k_0^2(\epsilon_{ri}-1)$$

$g_i(s)$ and s are related by ([8], Cap. 2)

$$g_i^2(s) - s^2 = k_0^2(\epsilon_{ri}-1)$$

$$h^2(s) = k_0^2 - s^2$$

The integrals $G_{ij}(\tilde{s})$, $I_{ij}(s,\tilde{s})$ and I_{ij} follow from $F_{ij}(\tilde{s})$, $H_{ij}(s,\tilde{s})$ and H_{ij}, respectively by replacing $\epsilon_i(x)$ by $\epsilon_j(x)$.

The system of four equations (5-8) is a set of integral equations in R, T, $B_1(s)$ and $B_2(s)$ that can be solved by a suitable numerical method.

IV. Moment Method Solution

To put the system to be solved in an appropriate form for the Method of Moments, let the unknown spectral density $B_i(s)$ be represented by the following series,

$$B_i(s) = \sum_{n=1}^{N} b_n^{(i)}f_n(s), \quad i=1,2 \quad (16)$$

where $f_n(s)$ are pulse functions, chosen as testing functions, and defined as follows:

$$f_n(s) = P(s-s_n) = \begin{cases} 1, & \text{for } |s-s_n| < \Delta s/2 \\ 0, & \text{for } |s-s_n| > \Delta s/2 \end{cases} \quad (17)$$

where Δs is the width of the pulse functions and s_n is the n^{th} pulse function's midpoint:

$$s_n = (n-1/2)\Delta s$$

$$\Delta s = k_0/N_0$$

and

$$K = s_N + \Delta s/2$$

where N is a suitable number of points, usually larger than N_0, the last value of n in which $h(s_{n-1})$ is still real. K is a large number that replaces infinity in the integrals of (5-8). The optimal values of N and N_0 are dictated by the convergence of the solution. For $n \geq N_0$, $h(s_n)$ is pure imaginary, giving rise to the evanescent modes.

By using the expansion (16) the equations (5-8) become,

$$\sum_{n=1}^{N} b_n^{(1)} P(\tilde{s} - s_n)/h(\tilde{s}) =$$

$$TF_{12}(\tilde{s}) + \sum_{n=1}^{N} b_n^{(2)} \int_0^K P(s - s_n) H_{12}(s, \tilde{s}) ds/h(s) \quad (18)$$

$$-\sum_{n=1}^{N} b_n^{(1)} P(\tilde{s} - s_n) N_1^2(\tilde{s}) =$$

$$Th_2 G_{12}(\tilde{s}) + \sum_{n=1}^{N} b_n^{(2)} \int_0^K P(s - s_n) I_{12}(s, \tilde{s}) ds \quad (19)$$

$$(I+R)N_1^2 = TH_{12} + \sum_{n=1}^{N} b_n^{(2)} \int_0^K P(s - s_n) G_{21}(s) ds/h(s) \quad (20)$$

$$(I-R)N_1^2 = Th_2 I_{12} + \sum_{n=1}^{N} b_n^{(2)} \int_0^K P(s-s_n) F_{21}(s) ds \quad (21)$$

If one uses the *point-matching method*, a suitable inner product is defined as follows,

$$< w_m, L(f_n) >= \int_0^K \delta(\tilde{s} - s_m) L(f_n) d\tilde{s}$$

where w_m, the weighting function, is given by $w_m = \delta(\tilde{s} - s_m)$, $L(f_n)$ is a linear operator, and f_n is the *unknown response* to be determined.

Thus, multiplying (21) by $\delta(\tilde{s} - s)$ and integrating over $\tilde{s}$ from 0 to K gives

$$b_m^{(1)} N_1^2(s_m) = TF_{12}(s_m) h(s_m) + h(s_m) \sum_{n=1}^{N} b_n^{(2)} l_{mn} \quad (22)$$

$$-b_m^{(1)} N_1^2(s_m) = TG_{12}(s_m) h_2 + \sum_{n=1}^{N} b_n^{(2)} m_{mn} \quad (23)$$

$$(I+R)N_1^2 h_1 = TH_{12} h_1 + \sum_{n=1}^{N} b_n^{(2)} l_{0n} \quad (24)$$

$$(I-R)N_1^2 h_1 = TI_{12} h_2 + \sum_{n=1}^{N} b_n^{(2)} m_{0n} \quad (25)$$

where l_{mn}, m_{mn}, l_{0n}, m_{0n} are defined as

$$l_{mn} = \int_{\Delta s_n} H_{12}(s, s_m) ds/h(s) \quad (26)$$

$$m_{mn} = \int_{\Delta s_n} I_{12}(s, s_m) ds \quad (27)$$

$$m_{0n} = \int_{\Delta s_n} G_{12}(s) ds/h(s) \quad (28)$$

$$m_{0n} = \int_{\Delta s_n} F_{21}(s) ds \quad (29)$$

where $\Delta s_n = (s_n - \frac{1}{2}\Delta s, s_n + \frac{1}{2}\Delta s)$.

Because of the properties of the pulse functions the range of these integrals were changed to 'local' range where each integral is performed over each pulse alone, Fig. 2. The above integrals cannot be solved in closed form. An approximate procedure is to expand part of the integrand that does not contain a function of the type $1/(s^2 - f^2)$ in a Taylor series about $s = s_n$, the midpoint of the range of integration. It is sufficient to consider only two terms of the expansion because the range of integration is or can be made small. This approximation is valid only for points where $h(s)$ does not vanish. Points very close to $s = k_0$ would give poor approximations.

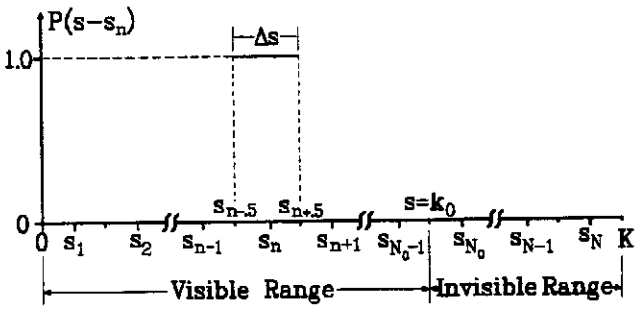

Figure 2: Pulse Function for N Points.

V. Power Considerations

Power in the Surface Wave

The power carried by the dominant mode surface wave (per unit length in the $y-$direction) for the upper half of the slab waveguide is

$$P_s = \frac{1}{2} \mathrm{Re} \int_0^\infty E_x H_y^* dx \quad (30)$$

where 'Re' means 'Real part of '. For TM modes the surface wave H field is given by

$$H_y(x, z) = A h_y(x) e^{-j h_z z} \quad (31)$$

where A is the mode amplitude. The '$\pm$' suffix for the wave number h has the following meaning

$$h_+ = h \quad \text{(forward wave)}$$

$$h_- = h \quad \text{(reflected wave)}$$

Moreover from Maxwell Equations,

$$E_x = \frac{1}{\omega\epsilon(x)}\frac{\partial}{\partial z}H_y = \frac{h_\pm}{\omega\epsilon_0\epsilon(x)}H_y(x,z) \tag{32}$$

Putting (31) and (32) into (30) gives

$$P_s = \frac{h_\pm}{2\omega\epsilon_0}|A|^2\int_0^\infty \frac{1}{\epsilon(x)}|h_y(x)|^2dx \tag{33}$$

Therefore the total power carried by the even TM_0 mode is

$$P_s = \frac{Z_0 h_\pm}{4k_0}|A|^2N^2 \tag{34}$$

where N is the discrete normalization factor given in (12), $Z_0 = \sqrt{\mu_0/\epsilon_0} \cong 120\pi\Omega$.

The Radiated Power

The total power of the radiating field for the upper half region is defined as

$$P_{\text{rad}} = \frac{1}{2}\int_0^\infty P(\theta)d\theta \tag{35}$$

where $P(\theta)$, the angular power density per unit width in the $y-$direction, is defined by

$$P(\theta)d\theta = Z_0|H_y(\rho,\theta)|^2, \quad [\rho\to\infty] \tag{36}$$

where ρ is the distance to the far field observation point from the origin and θ is the angle between the direction of and the $z-$axis, measured from the latter (Fig. 1).

For TM pseudo-modes the pseudo-surface wave H field is given by

$$H_y(x,z) = \frac{1}{2}\int_0^\infty \frac{B(s)}{h_\pm(s)}h_y(x,s)\,e^{-jh_\pm(s)z}\,ds \quad \text{(cf.(31))} \tag{37}$$

where $B(s)$ is the unknown spectral density and $h_y(x,s)$, the transverse function for the continuous TM mode field is given by

$$h_y(x,s) = [v(s) - jw(s)]\,e^{-js(x-b)}, \quad [x \geq b] \tag{38}$$

where $v(s)$ and $w(s)$ are given by (14) and (15), respectively. Notice that in writing (37) one considered only the outgoing term of the pseudo-mode solution because the incoming one makes no contribution in the upper half region. It is possible to show that the incoming term leads to an expression for the radiated power in the lower half region, which, by symmetry can be deduced from that for the upper half region.

The integral above - (37), cannot be evaluated in closed form. Fortunately, for radiation problems, the primary interest is with the far field and so one can apply asymptotic integration techniques such as the saddle-point method. It is convenient to make the following changes of variables,

$$x - b = \rho\sin(\theta), \qquad z = \rho\cos(\theta) \tag{39}$$

$$s = k_0\sin\gamma, \qquad h(s) = k_0\cos(\gamma) \tag{40}$$

since

$$\rho^2 = x^2 + z^2 \tag{41}$$

$$k_0^2 = s^2 + h^2(s) \tag{42}$$

In terms of the new variables, (37) can be written, for $(0 < \theta < \pi)$

$$H_y(\rho,\theta) = \frac{1}{2}\int_C B(k_0\sin\gamma, \pm k_0\cos\gamma)$$
$$[v(k_0\sin\gamma) - jw(k_0\sin\gamma)]\,e^{\mp jk_0\rho\cos(\gamma\mp\theta)}\,d\gamma \tag{43}$$

where the upper and lower signs in the exponential term and in the function B stand for $z \geq 0$ and $z \leq 0$, respectively. C is the integral path for the saddle-point method of integration.

For $z > 0$ $(\pi/2 \leq \theta < \pi)$ the saddle point is $\tilde{\theta} = \theta$ and for $z < 0$ $(\pi/2 \leq \theta < \pi)$ the saddle point is $\tilde{\theta} = \pi - \theta$ ([9],p.108,9).

For very large $k_0\rho$, that is, for points far from the discontinuity, the following asymptotic expression is obtained

$$H_y(\rho,\tilde{\theta}) \cong \sqrt{\frac{\pi}{2k_0\rho}}B(k_0\sin\theta, \pm k_0\cos\theta)$$
$$[v(k_0\sin\theta) - jw(k_0\sin\theta)]\,e^{-j(k_0\rho-\pi/4)} \tag{44}$$

Thus the far field of (44) is a diverging cylindrical wave satisfying the radiation condition, with pattern given by

$$Q(\tilde{\theta}) = B(\tilde{\theta})[v(\tilde{\theta}) - jw(\tilde{\theta})] \tag{45}$$

In view of (44) one writes

$$\left|H_y(\rho,\tilde{\theta})\right|^2 \cong \frac{\pi}{2k_0\rho}|B(\theta)|^2\,[v^2(\theta) + w^2(\theta)] \tag{46}$$

and consequently, with reference to (36),

$$P(\tilde{\theta}) = \frac{Z_0}{4k_0}|B(\tilde{\theta})|^2N^2(\tilde{\theta}) \tag{47}$$

where $N^2(\tilde{\theta})$ is given by

$$N^2(\tilde{\theta}) = \frac{\pi}{2}[v^2(\tilde{\theta}) + w^2(\tilde{\theta})] \tag{48}$$

Substituting (47) into (35) gives

$$P_{\text{rad}} = \frac{Z_0}{4k_0}\int_0^{\infty} |B(\tilde{\theta})|^2 N^2(\tilde{\theta}) d\tilde{\theta} \qquad (49)$$

More explicitly, in terms of s

$$P_{\text{rad}} = \frac{Z_0}{4k_0}\int_0^{\infty} |B(s)|^2 N^2(s) ds/h(s) \qquad (50)$$

Notice that $ds/h(s) = \tilde{\theta}$, due to the change of variable.

The forward and backward radiation powers are included in (49) when $\tilde{\theta}$ is properly replaced; thus when $\tilde{\theta}$ runs from 0 to π, é has two stationary values and consequently the integrand is split into two terms, corresponding to the forward and back scattered radiation each associated with the same value of s.

The power pattern is then

$$Q(\tilde{\theta}) = |B(\tilde{\theta})|^2 N^2(\tilde{\theta}), \quad [0 < \tilde{\theta} < \pi] \qquad (51)$$

VI. Numerical Results and Discussion

For numerical calculation purposes the incident power is set to unity. Consequently, the transmitted, reflected, and radiated powers are normalized with respect to the incident power. They are in the convenient forms given as follows :

$$P_{\text{trans}} = T^2 \left(\frac{h_2 N_2^2}{h_1 N_1^2}\right) \qquad (52)$$

$$P_{\text{ref}} = R^2 \qquad (53)$$

$$P_{\text{rad}} = \frac{1}{h_1 N_1^2}\sum_{n=1}^{N_0}\left[\left|b_n^{(1)}\right|^2 N_1^2(s_n) + \left|b_n^{(2)}\right|^2 N_2^2(s_n)\right]\frac{\Delta s}{h(s_n)} \qquad (54)$$

The superscript upon b_n and the subscript in the other variables refer to the medium on the left '1' and on the right '2'.

The actual total power (incident plus scattered) for the slab waveguide is double the value obtained here because one is considering only half the slab.

The backward and forward power patterns are written as functions of θ_n and $b_n^{(1)}$ and $b_n^{(2)}$ as

$$Q_1(\theta_n) = |b_n^{(1)}|^2 N_1^2(\theta_n), \quad [\pi/2 < \theta_n \leq \pi] \qquad (55)$$

$$Q_2(\theta_n) = |b_n^{(2)}|^2 N_2^2(\theta_n), \quad [0 < \theta_n \leq \pi/2] \qquad (56)$$

where

$$\theta_n = \begin{cases} \sin^{-1}(s_n/k_0), & [0 < \theta_n \leq \pi/2] \\ \pi - \sin^{-1}(s_n/k_0), & [\pi/2 \leq \theta_n < \pi] \end{cases} \qquad (57)$$

Notice that, in principle, the total scattered power equals 1 and that the following relation must hold

$$P_{\text{trans}} + P_{\text{ref}} + P_{\text{rad}} = 1 \qquad (58)$$

The expression above is useful to indicate whether the calculations performed are or are not accurate. Of course this relation is not a sufficient condition for the solution of the problem.

In the following subsection the solutions of the system of equations (22-25) are presented for several selected cases.

Convergence

Curves showing the variation of the transmitted, reflected, and radiated power with changes of the slab thickness in the right region are shown in Fig. 3. These plots were obtained by varying $2b_2/\lambda_0$ from .001 to 0.40. The conservation of energy was verified in all cases with $N = 48$ points and $N_0 = 24$ points. These results show that there are no problems of convergence for changes in b_2, even for very small values. It is worth remarking that the radiated energy is very small, unless large steps are considered (small values of b_2). For example, when $2b_2/\lambda_0 = 0.001$ almost all energy is radiated and the reflected energy is very small.

Power Patterns

The main concern here is the radiation characteristics due to the step in the geometry. Several cases were considered in order to show these properties. Curves of Fig. 4 and 5 show the pattern characterists for some particular cases. One can notice that the smaller the dimension of the slab at the right side the closer to $\theta = 0°$ is the peak of the radiated field. The error with respect to the total power involved in the calculations above is less then 1% for all cases with $N = 48$ and $N_0 = 24$.

V. Conclusion

The Moment Method applied throughout this work has been shown to be accurate, efficient, and the results are very convincing for many practical cases of axial discontinuities in dielectric waveguide structures. The formulation of the field equations are exact and straightforward. On the other hand one concludes that the truncated number of equations N and the number of equations in the visible range N_0 play a very important role in the convergence of the solution. For most specific cases the number of points in the invisible range need not be large.

The technique applied in this work can also be used for the slab and rod (TM_{01}) waveguide with ascending steps in the geometry. Steps in the dielectric medium are also possible and the formulation is slightly simpler. Mixed cases can also be treated with some increase in complexity of mathematical handling.

The method has to be changed in the case of free-end structures ($b_2 = 0$) since one gets more equations than needed because T becomes zero (see set of equations (22-25)). That is the reason the system gets unstable as b_2 approaches the air.

REFERENCES

[1] H. M. Barlow and J. Brown. *Radio Surface Waves.* Oxford University Press, Amen House, London, 1962.

[2] Alan F. Kay. "Scattering of a Surface Wave by a Discontinuity in Reactance" *IRE Trans. Antennas and Prop.*, AP-7:22-31, (Jan) 1959.

[3] Elmer L. Johansen. "Surface Wave Scattering by a Step". *IEEE Transactions on Antennas and Propagation*, AP-15:442+6, May 1967.

[4] Dietrich Marcuse. "Radiation Losses of Tapered Dielectric Slab Waveguides". *Bell System Technical Journal*, 49:273+17, February 1963.

[5] S. Nemoto and T. Makimoto. "Radiation Loss Caused by Discontinuities in a Dielectric Slab Waveguide". *Wave Electronics*, 3:249+13, March 1978.

[6] A. Ittipiboon and M. Hamid. "Scattering of Surface Waves at a Slab Waveguide Discontinuity" *Proc. IEEE*, 126-#9:798-804,(Sep) 1979.

[7] Koichi Hirayama and Manasori Koshiba. "Numerical analysis of arbitrarily shaped discontinuities between planar dielectric waveguides with different thicknesses" *IEEE Trans. Microwave Theory Tech.*, MTT-38:260-264, (Mar) 1990.

[8] Creso S. da Rocha. **An Investigation of the Scattering of Surface Waves at Dielectric Waveguide Discontinuities by the Moment Method**, Ph.D. Thesis, Dept. of Elect. Eng'g, The University of Waterloo, Waterloo, Ontario, Canada (1980).

[9] V. V. Shevchenko **Continuous Transitions in Open Waveguides**, The Golem Press, Boulder, Colorado, 1971.

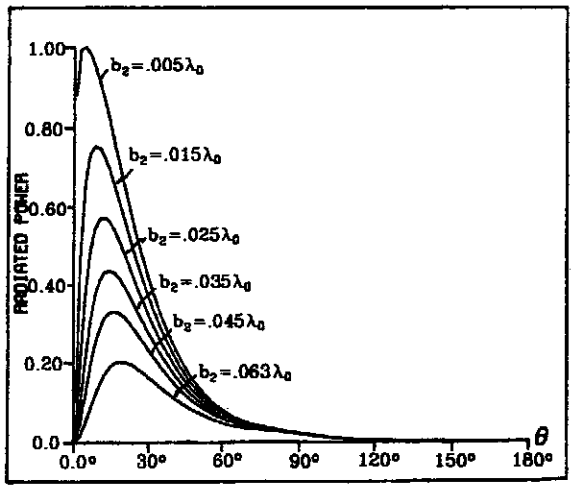

Figure 4: The Power Pattern for $b_2/\lambda_0 = 0.005...0.063$ with $\epsilon_{r1} = \epsilon_{r2} = 2.56$.

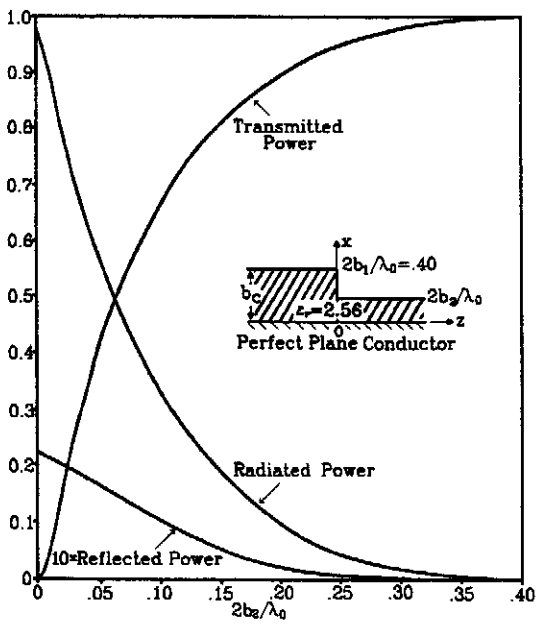

Figure 3: Power vs. the Slab Thickness in the Right Region for $2b_1 = .4\lambda_0$ and $\epsilon_{r1} = \epsilon_{r2} = 2.56$.

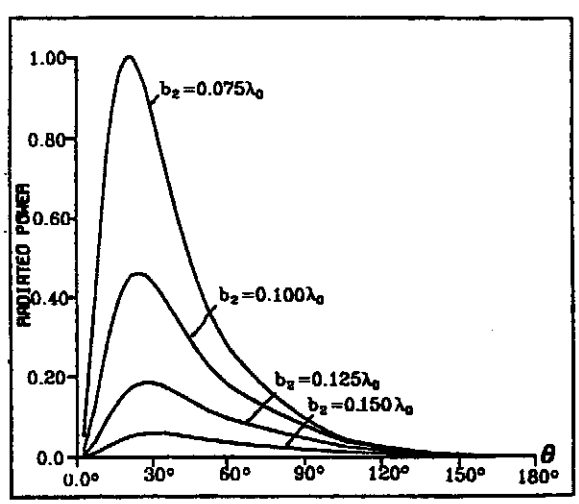

Figure 5: The Power Pattern for $b_2/\lambda_0 = 0.075...0.150$ with $\epsilon_{r1} = \epsilon_{r2} = 2.56$.